

Note to readers with disabilities: *EHP* strives to ensure that all journal content is accessible to all readers. However, some figures and Supplemental Material published in *EHP* articles may not conform to [508 standards](#) due to the complexity of the information being presented. If you need assistance accessing journal content, please contact ehp508@niehs.nih.gov. Our staff will work with you to assess and meet your accessibility needs within 3 working days.

Supplemental Material

Hepatic Tumor Formation in Adult Mice Developmentally Exposed to Organotin

Tiffany A. Katz, Sandra L. Grimm, Akhilesh Kaushal, Jianrong Dong, Lindsey S. Treviño, Rahul K. Jangid, Adriana V. Gaitán, Jean-Philippe Bertocchio, Youchen Guan, Matthew J. Robertson, Robert M. Cabrera, Milton J. Finegold, Charles E. Foulds, Cristian Coarfa, and Cheryl Lyn Walker

Table of Contents

Figure S1. Gapdh levels are similar across treatment groups in 45 week-old male mice developmentally exposed to tributyltin. (A). Gapdh mRNA threshold cycle (Ct) values are presented as median +/- interquartile (IQ)1-IQ3, n = 5 – TBT liver (orange circles), n = 7 – TBT-exposed adenoma (green squares). **(B).** GAPDH protein intensity is presented as mean +/- standard error of the mean (SEM) (VEH liver (hatched bar) – n = 6, TBT liver (solid orange bar) – n = 5, TBT-exposed adenoma (solid green bar) – n = 7). Ttests were performed and no statistically significant differences were noted. (TBT = tributyltin, VEH = vehicle).

Figure S2. Animal weights and comparisons by parity in tributyltin-exposed pups. (A). Dam weights in grams are presented at the start of breeding for each pregnancy (left, n = 8 for tributyltin (TBT, open bars) and n = 5 for vehicle (VEH, hatched bars)), sire weights are presented at the time of euthanasia (middle, n = 5). **(B).** Values for alanine aminotransferase (ALT) and aspartate aminotransferase (AST) activities (n = 3 - P1 with adenomas, n = 4 – P2 with adenomas, n = 2 – P1 without adenomas, n = 3 – P2 without adenomas), as well as adipose surface area by magnetic resonance imaging (MRI) (n = 2 – P1, n = 2 – P2) (NOTE: MRI in females was conducted only on animals from pregnancy 1) and Oil Red O (ORO) staining (n = 8 for P1 males, n = 2 for P2 males, n = 6 for P1 females, n = 3 for P2 females) are presented per pregnancy in TBT-exposed pups. Bars represent the mean +/- standard error of the mean (SEM); ttests were performed and no significant differences were noted. In all graphs P1 = pregnancy 1 (hatched bars), and P2 = pregnancy 2 (solid bars). Table S1 details information on n and litter.

Figure S3. Weights of mice developmentally exposed to vehicle or tributyltin over time.

Bodyweights in grams are presented as mean +/- standard error of the mean (SEM) (n = 5 in both female (F) groups ('TBT F' - open red triangles and 'VEH F' - closed red triangles) and males (M) who never developed tumors ('TBT M' open blue circles); n = 6 for VEH-exposed males ('VEH M' closed blue circles); and n = 7 for TBT-exposed males who developed tumors (TM) ('TBT TM' open blue squares)). Repeated measures analysis of variance (ANOVA) was used to determine statistical differences between treatment groups (males and females were analyzed separately) and no statistically significant differences were noted.

Figure S4. Alanine aminotransferase (ALT) and aspartate aminotransferase (AST) activity levels in serum from developmentally exposed vehicle- and tributyltin-exposed 45 week-old male mice. AST and ALT activity levels are presented in mU/mL. Bars represent the mean +/- standard error of the mean (SEM) and a one-way analysis of variance (ANOVA) was performed to ascertain significance (* = $p < 0.05$, NS = not significant). "A" = TBT-exposed mice presenting with an adenoma (solid green bar, n = 7), "V" = vehicle-exposed liver (hatched bar, n = 6), "T" = tributyltin-exposed liver from animals that did not develop tumors (solid orange bar, n = 5). Table S1 details information on n and litter.

Figure S5. Vehicle-exposed adenoma displays a more differentiated phenotype with a higher amount of lipid present. Representative images of hematoxylin and eosin staining of a vehicle (VEH)-exposed liver and a VEH-exposed adenoma from a separate male mouse at 45 weeks of age.

Figure S6. Differential gene expression in tributyltin-exposed adenomas versus vehicle-exposed liver samples. (A). Hierarchical clustering of samples from male mice using differentially expressed genes (FDR adjusted p-value < 0.05 with a fold change exceeding 2x). (B). Principal component analysis of adenoma and vehicle treated liver RNA-seq data in panel A. Blue triangles depict VEH-exposed liver and green squares depict TBT-exposed adenoma. (C). Quantitative PCR validation of eight genes spanning the top 2% of differentially expressed genes identified in the RNA-seq analysis in panel A. (D). Quantitative PCR validation of the five most repressed *Mup* genes as identified in the RNA-seq analysis in panel A. In all graphs, 'V' (blue circles) depict VEH-exposed liver and 'A' (green squares) represent TBT-exposed adenomas, the median +/- interquartile (IQ)1-IQ3 are presented and Mann-Whitney U tests were performed to ascertain significance (** = $p < 0.01$, *** = $p < 0.001$). Table S1 details information on n and litter.

Figure S7. Genes differentially expressed in tributyltin-promoted liver adenomas overlap with common cancer related pathways in the Hallmark and KEGG pathway databases. An overrepresentation analysis (ORA) was conducted using the genes differentially expressed in the TBT-exposed adenomas over TBT-exposed liver tissue (A), or VEH-exposed liver tissue (B) (closed bars = increased genes in adenomas, open bars = decreased genes in adenomas) against the Hallmark and KEGG pathway databases as compiled by MSigDB.

Figure S8. Differentially expressed genes in tributyltin-induced display an inverse expression in comparison to GHR signatures. Expression levels of significantly ($q < 0.05$) differentially expressed genes in the tributyltin (TBT)-induced adenoma over TBT-exposed liver (**A**), or vehicle-exposed liver (**B**) (open bars = GHR signature, solid bars = adenoma signature) signature display an inverse expression in the GHR gene signature. Bars represent fold change (Log_2) of each gene in the RNA-seq data. Asterisks indicate STAT5 direct target genes determined from analysis of publicly available STAT5 mouse liver ChIP-seq dataset.

Additional File- Excel Document

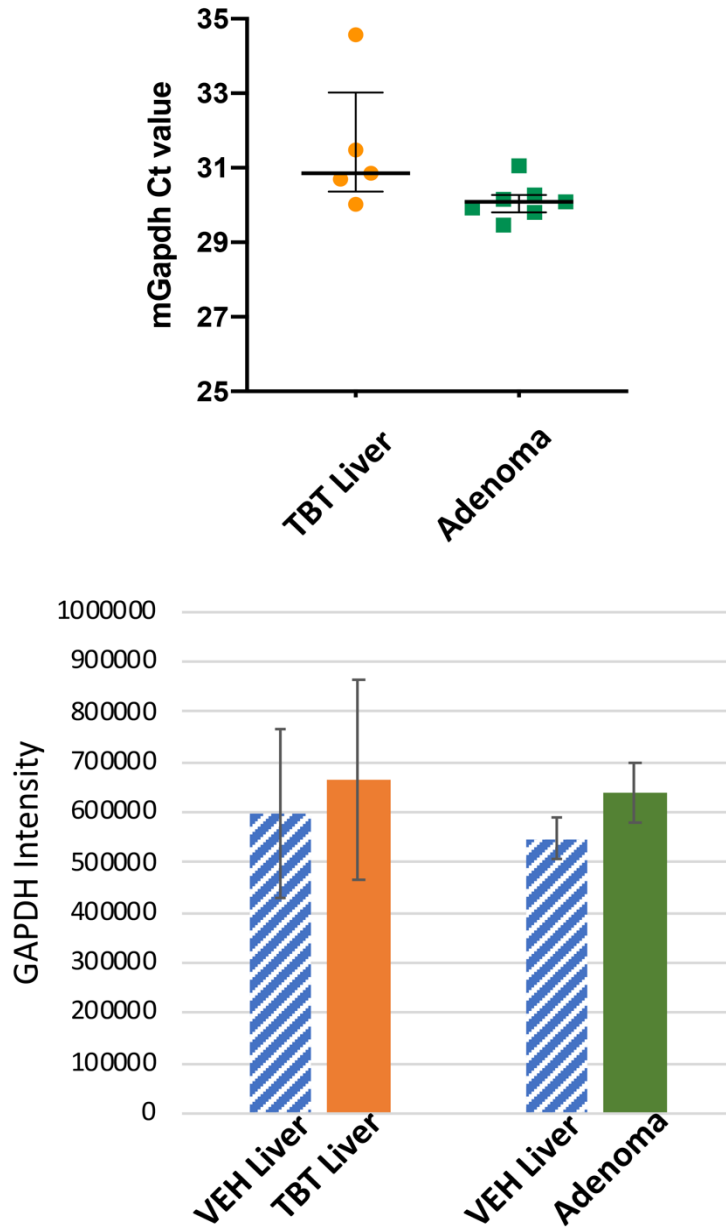


Figure S1. Gapdh levels are similar across treatment groups in 45 week-old male mice developmentally exposed to tributyltin. (A). Gapdh mRNA threshold cycle (Ct) values are presented as median +/- interquartile (IQ)1-IQ3, n = 5 – TBT liver (orange circles), n = 7 – TBT-exposed adenoma (green squares). **(B).** GAPDH protein intensity is presented as mean +/- standard error of the mean (SEM) (VEH liver (hatched bar) – n = 6, TBT liver (solid orange bar)– n = 5, TBT-exposed adenoma (solid green bar) – n = 7). Ttests were performed and no statistically significant differences were noted. (TBT = tributyltin, VEH = vehicle)

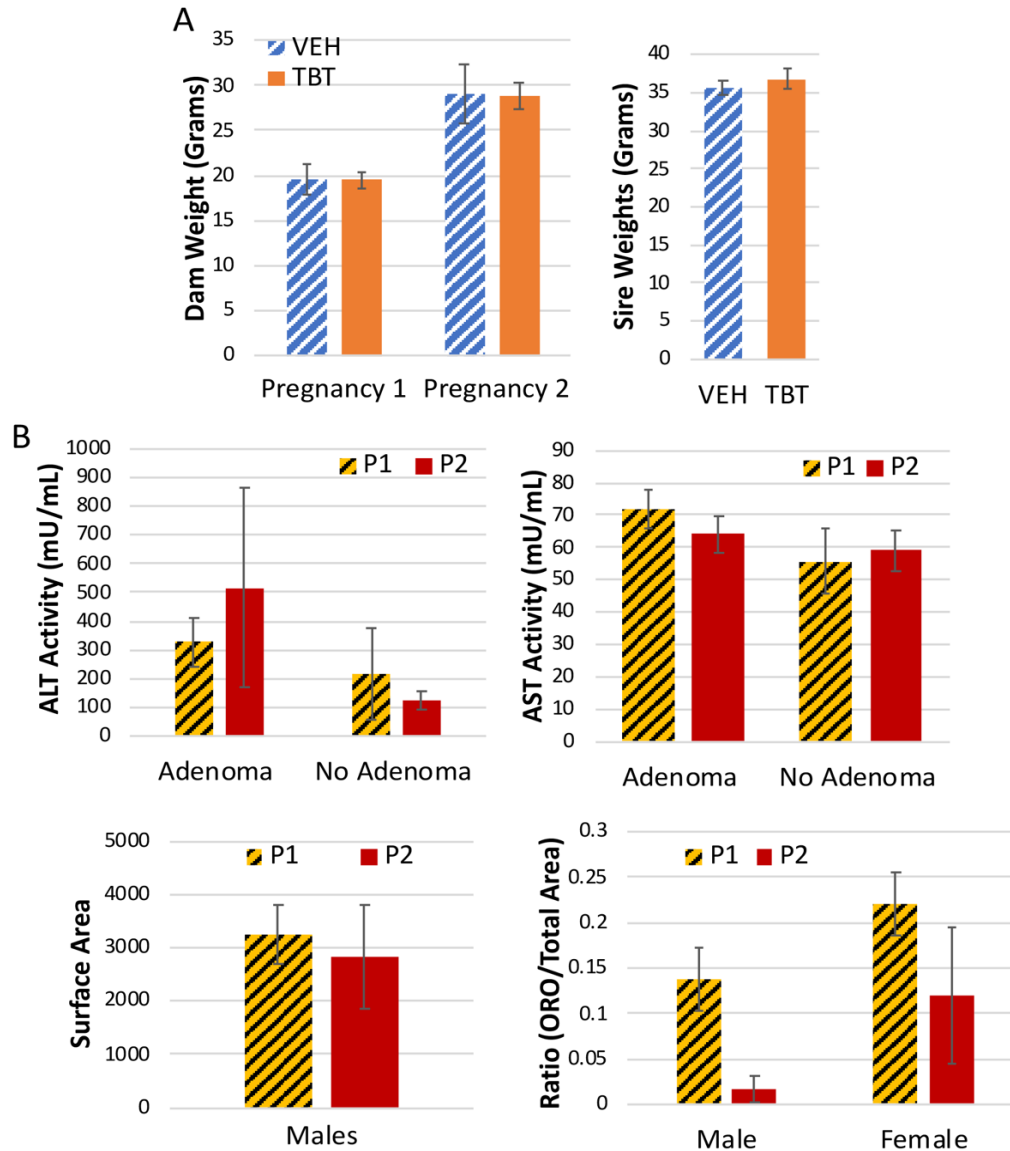


Figure S2. Animal weights and comparisons by parity in tributyltin-exposed pups. (A). Dam weights in grams are presented at the start of breeding for each pregnancy (left, n = 8 for tributyltin (TBT, open bars) and n = 5 for vehicle (VEH, hatched bars)), sire weights are presented at the time of euthanasia (middle, n = 5). **(B).** Values for alanine aminotransferase (ALT) and aspartate aminotransferase (AST) activities (n = 3 - P1 with adenomas, n = 4 - P2 with adenomas, n = 2 - P1 without adenomas, n = 3 - P2 without adenomas), as well as adipose surface area by magnetic resonance imaging (MRI) (n = 2 - P1, n = 2 - P2) (NOTE: MRI in females was conducted only on animals from pregnancy 1) and Oil Red O (ORO) staining (n = 8 for P1 males, n = 2 for P2 males, n = 6 for P1 females, n = 3 for P2 females) are presented per pregnancy in TBT-exposed pups. Bars represent the mean +/- standard error of the mean (SEM); ttests were performed and no significant differences were noted. In all graphs P1 = pregnancy 1 (hatched bars), and P2 = pregnancy 2 (solid bars). Table S1 details information on n and litter.

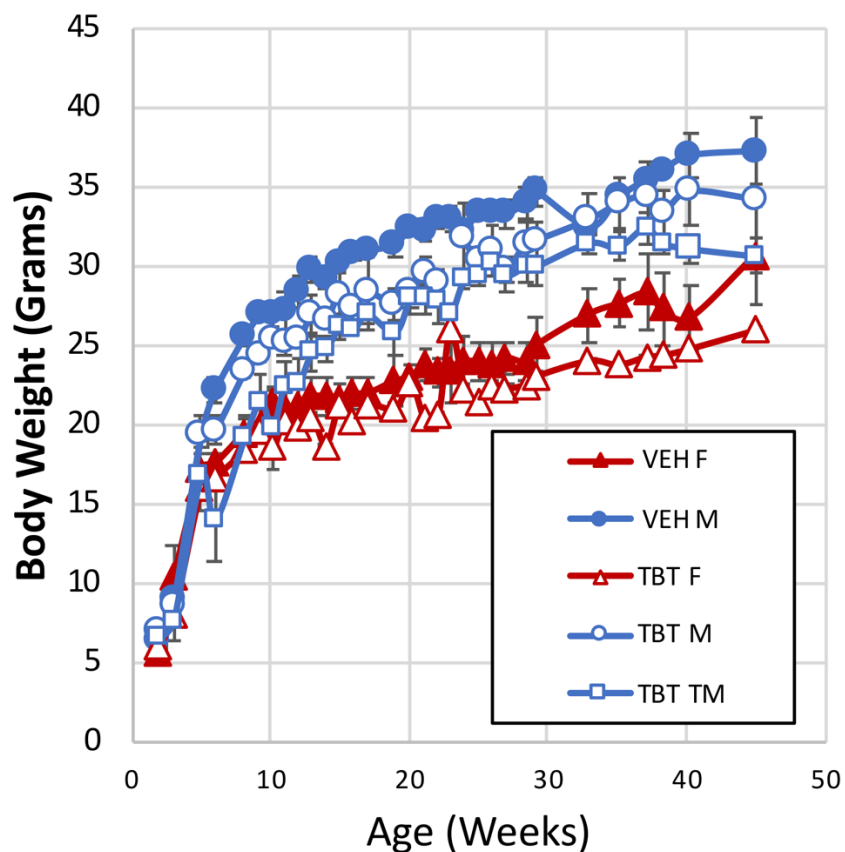


Figure S3. Weights of mice developmentally exposed to vehicle or tributyltin over time. Bodyweights in grams are presented as mean +/- standard error of the mean (SEM) (n = 5 in both female (F) groups ('TBT F' - open red triangles and 'VEH F' - closed red triangles) and males (M) who never developed tumors ('TBT M' open blue circles); n = 6 for VEH-exposed males ('VEH M' closed blue circles); and n = 7 for TBT-exposed males who developed tumors (TM) ('TBT TM' open blue squares)). Repeated measures analysis of variance (ANOVA) was used to determine statistical differences between treatment groups (males and females were analyzed separately) and no statistically significant differences were noted.

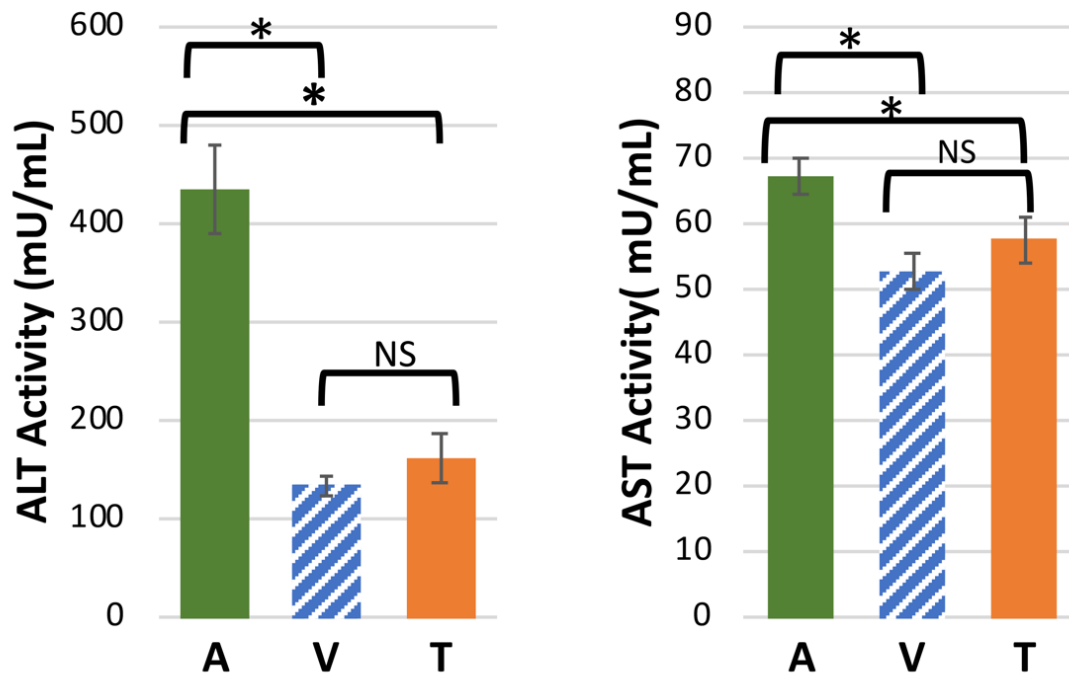
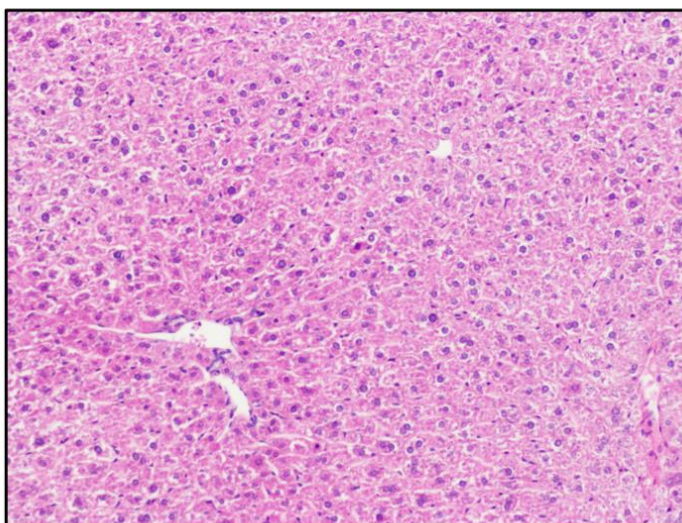


Figure S4. Alanine aminotransferase (ALT) and aspartate aminotransferase (AST) activity levels in serum from developmentally exposed vehicle- and tributyltin-exposed 45 week-old male mice. AST and ALT activity levels are presented in mU/mL. Bars represent the mean +/- standard error of the mean (SEM) and a one-way analysis of variance (ANOVA) was performed to ascertain significance (* = $p < 0.05$, NS = not significant). "A" = TBT-exposed mice presenting with an adenoma (solid green bar, $n = 7$), "V" = vehicle-exposed liver (hatched bar, $n = 6$), "T" = tributyltin-exposed liver from animals that did not develop tumors (solid orange bar, $n = 5$). Table S1 details information on n and litter.

VEH Liver



VEH Adenoma

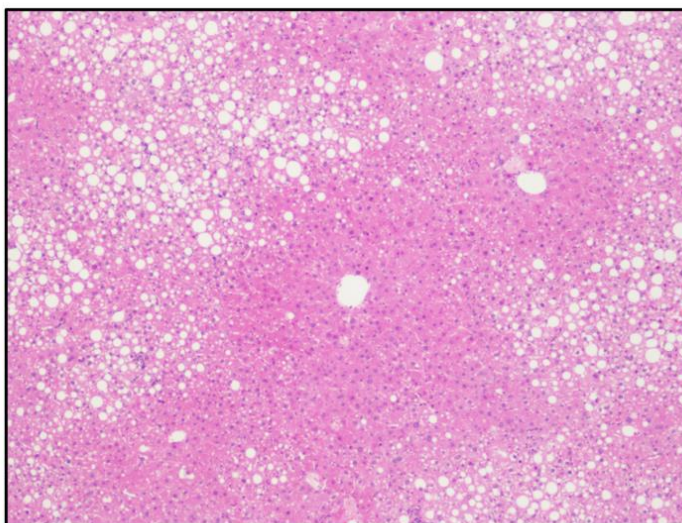


Figure S5. Vehicle-exposed adenoma displays a more differentiated phenotype with a higher amount of lipid present. Representative images of hematoxylin and eosin staining of a vehicle (VEH)-exposed liver and a VEH-exposed adenoma from a separate male mouse at 45 weeks of age.

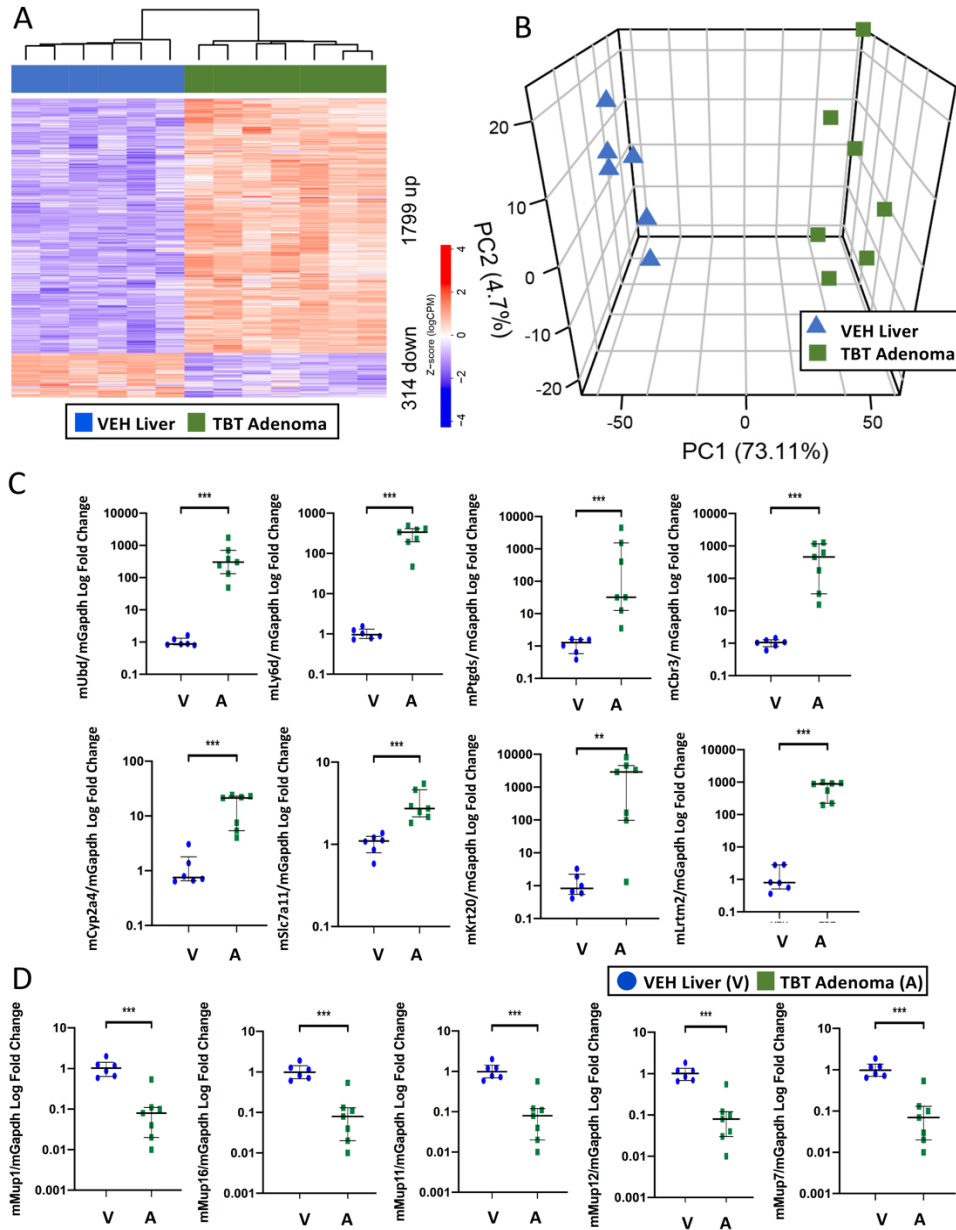
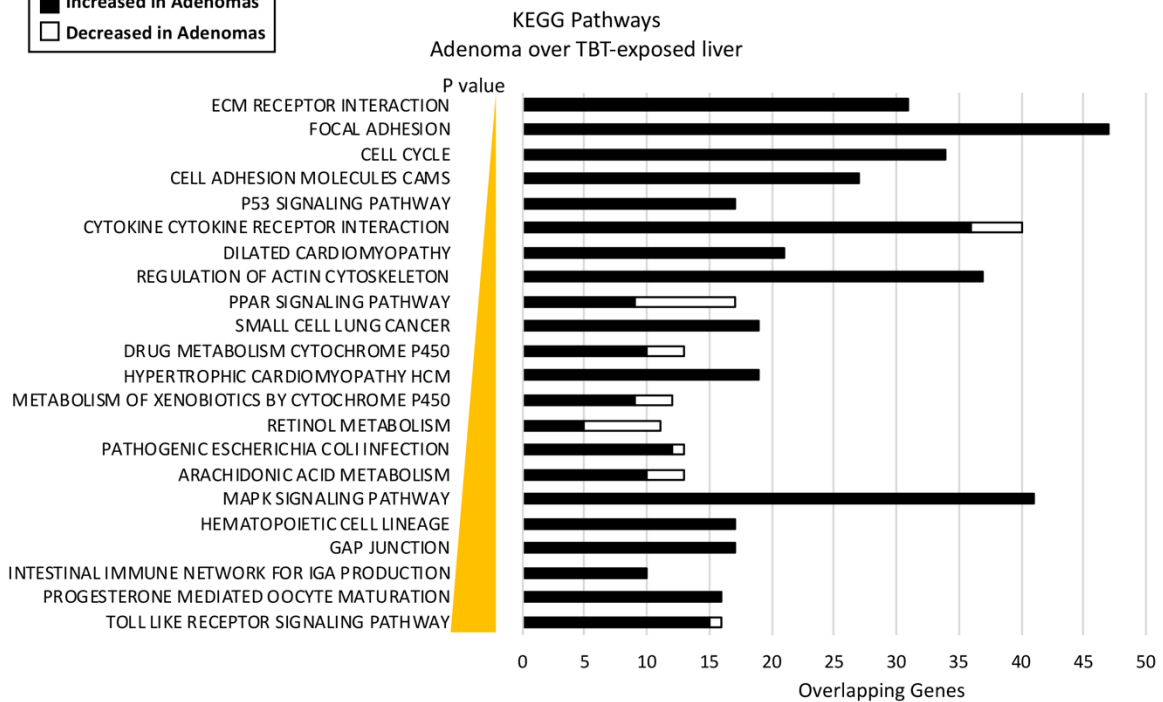
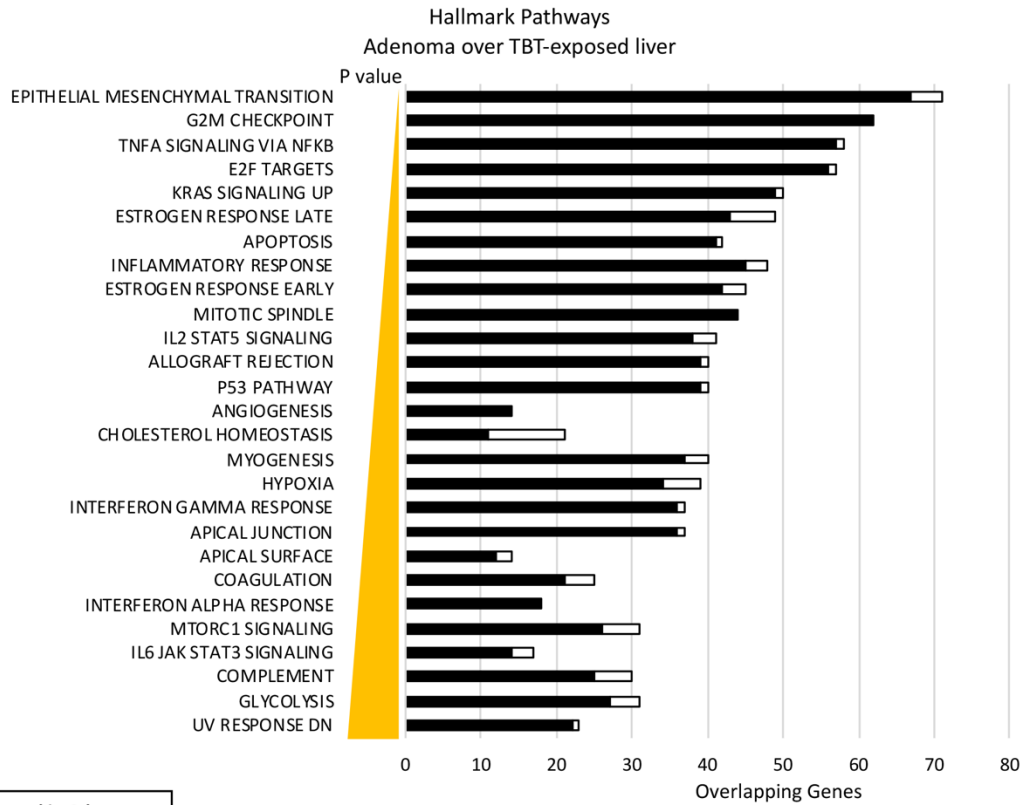


Figure S6. Differential gene expression in tributyltin-exposed adenomas versus vehicle-exposed liver samples. (A). Hierarchical clustering of samples from male mice using differentially expressed genes (FDR adjusted p-value < 0.05 with a fold change exceeding 2x). **(B).** Principal component analysis of adenoma and vehicle treated liver RNA-seq data in panel A. Blue triangles depict VEH-exposed liver and green squares depict TBT-exposed adenoma. **(C).** Quantitative PCR validation of eight genes spanning the top 2% of differentially expressed genes identified in the RNA-seq analysis in panel A. **(D).** Quantitative PCR validation of the five most repressed *Mup* genes as identified in the RNA-seq analysis in panel A. In all graphs, 'V' (blue circles) depict VEH-exposed liver and 'A' (green squares) represent TBT-exposed adenomas, the median +/- interquartile (IQ)1-IQ3 are presented and Mann-Whitney U tests were performed to ascertain significance (** = p < 0.01, *** = p < 0.001). Table S1 details information on n and litter.



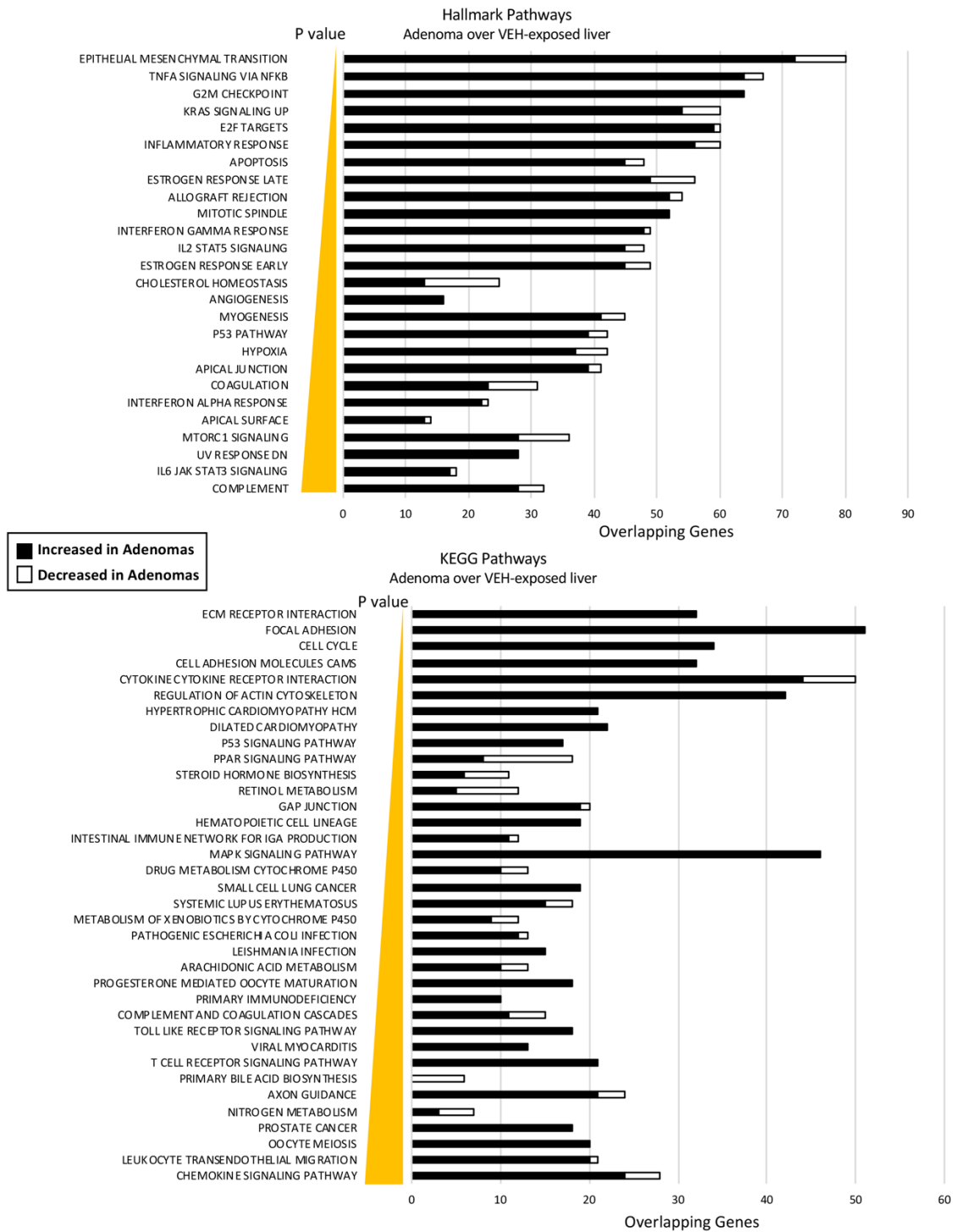


Figure S7. Genes differentially expressed in tributyltin-promoted liver adenomas overlap with common cancer related pathways in the Hallmark and KEGG pathway databases. An overrepresentation analysis (ORA) was conducted using the genes differentially expressed in the TBT-exposed adenomas over TBT-exposed liver tissue (A), or VEH-exposed liver tissue (B) (closed bars = increased genes in adenomas, open bars = decreased genes in adenomas) against the Hallmark and KEGG pathway databases as compiled by MSigDB.

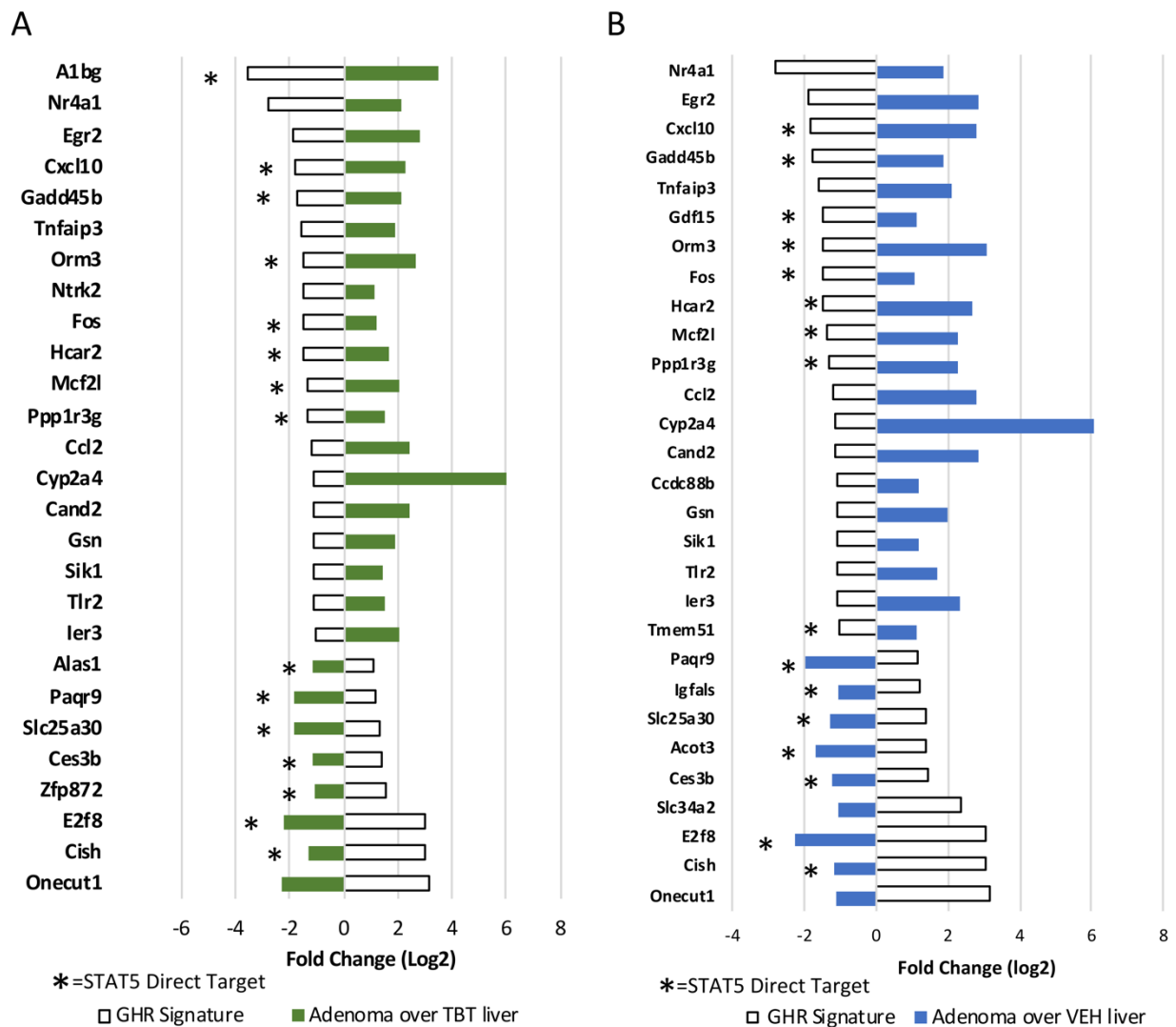


Figure S8. Differentially expressed genes in tributyltin-induced display an inverse expression in comparison to GHR signatures. Expression levels of significantly ($q < 0.05$) differentially expressed genes in the tributyltin (TBT)-induced adenoma over TBT-exposed liver (**A**), or vehicle-exposed liver (**B**) (open bars = GHR signature, solid bars = adenoma signature) signature display an inverse expression in the GHR gene signature. Bars represent fold change (Log_2) of each gene in the RNA-seq data. Asterisks indicate STAT5 direct target genes determined from analysis of publicly available STAT5 mouse liver ChIP-seq dataset.